IJICTR
International Journal of Information & Communication Technology Research

Volume 12- Number 1 – Winter 2020 (1 -10)

Performance Assessment of a Microwave Life-Detection System (MLDS): Modified Quadrature Receiver Versus a Harmonic Radar Architecture

Kamyar Abyar
Department of Electrical Engineering, University of Guilan, Rasht, Iran.
kamyar.abyar.l@gmail.com

Gholamreza Baghersalimi *
Department of Electrical Engineering, University of Guilan, Rasht, Iran.
bsalimi@guilan.ac.ir

Alireza Saberkari
Department of Electrical Engineering, University of Guilan, Rasht, Iran.
saberkari@guilan.ac.ir

Mahdi Nassiri
Department of Electrical Engineering, University of Guilan, Rasht, Iran.
nassirim12@yahoo.com

Received: 25 September 2019 - Accepted: 16 December 2019

Abstract—**Reliable detection of life under rubble and collapsed buildings after disasters like earthquake or air raid is the most important issue in life-detection process. In this paper, the performance of microwave life-detection system (MLDS) based on a continuous wave (CW) radar is analyzed from different aspects such as penetration depth, sensitivity, and total harmonic distortion (THD) of the output signal. A novel quadrature receiver as an appropriate architecture for the MLDS, and harmonic radar system as an alternative structure are proposed in order to resolve the well-known null point issue and improve the sensitivity of the system. Results show that by using these structures in the MLDS, the null points can be completely removed and hence the chance of detecting a trapped victim under the rubble can be improved considerably. Moreover, by using the harmonic structure, the received power in some distances away from the MLDS can be improved by 3 dB compared to that of the conventional systems. By examining different frequencies, 1.15 GHz (L-band) is found to be the most appropriate carrier frequency because of deeper penetration of about 5 meters in the rubble and 7 percent improved output signal THD compared to the previously designed X-band radars for the MLDS.**

Keywords-Microwave life-detection system; harmonic radar architecture; modified quadrature receiver; continuous wave radar; penetration depth, total harmonic distortion; heartbeat; respiration.

I. INTRODUCTION

Life-detection system using microwave Doppler radar was first introduced by K. M. Chen where an unmodulated continuous wave (CW) is transmitted to collapsed buildings and rubbles to find the probable targets [1]. The backscattered wave is phase modulated by displacement of the target's chest due to heartbeat and respiration. Microwave life-detection system (MLDS) extracts this information by appropriate demodulation techniques such as arctangent demodulation [2], complex signal demodulation (CSD) [3], etc.

It is shown in [4] that the backscattered wave is modulated in both amplitude and phase. However, since the phase variations are more linear and easier to detect, in most cases phase modulation of the received signal is used to detect the vibrations of body surface and displacements of the survivor's chest-wall.

* Corresponding Author

Although the MLDS could not be a replace for the conventional methods of life-detection, but can accurately detect the life of survivors if it is well designed. Moreover, by using pulse Doppler radars, the aforementioned system can be used to determine the distance between radar and the target. Also, the advantages and disadvantages of the frequency modulated continuous wave (FMCW) radar as the modulated scatterer technique was explained in [5]. The first designed system operated at the X-band of microwave frequencies with 10 GHz carrier frequency, but in order to reach higher depths of rubble, L or S band range of microwave frequencies are more suitable. This is because of the increase in signal attenuation at higher frequencies in a dielectric medium such as concrete, stone, brick or other building materials [4]. Rubble is an attenuating and nonhomogeneous medium because of existence of metal, water, etc. Snow, as a homogeneous material, is another medium that exists in avalanche scenarios. For this case, the designed MLDS is able to detect breathing through a 1.8 m thick snow barrier [6].

Despite many successfully designed life-detection systems, there are still several improvements to be achieved in the system performance. Issues such as random body movement (RBM) and static clutter are examples which can degrade sensitivity of the system and lead to a false detection. For example, in [3, 7] demodulation techniques were used to overcome the RMB problem.

A rescue system was proposed in [8] so that the backscattered signal was received by a patch antenna and then processed by Independent Component Analysis (ICA) method. A 60 GHz millimeter-wave MLDS was presented in [9] which used a clutter cancellation system with an attenuator and a phase shifter to avoid signal saturation in the receiver path. A compact portable MLDS was also proposed and fabricated in [10] at 1.15 GHz operating frequency which has the ability of accurately detecting vital life signals through highly dense materials of about 1.5 m in thickness and normal density materials of about 9 m in thickness. The authors used two individual horn antennas to reduce direct coupling between transmitter and receiver.

Sensitivity degradation of system caused by dependence of the received power to the nominal distance between the radar and target and null points issue was completely introduced in [11]. In addition, quadrature receiver was employed in [12] to overcome this problem in biomedical applications such as heartbeat measurements in clinics.

In this paper, quadrature receiver is used as the appropriate receiver architecture of the system. Also, a harmonic radar system is proposed for the MLDS for the first time. Both of these systems can be used to cancel the well-known null point problem of the Doppler radars and also achieve higher received power and hence improved sensitivity of the system. In previously designed life-detection systems, no fundamental theoretical analysis was performed to assess the effects of rubble on electromagnetic (EM) wave propagation and attenuation of the transmitted signal. In this paper, the effect of medium on the transmitted signal is analyzed in several cases to determine the received power in the presence of attenuating rubble. In order to compare system performance for different carrier frequencies, the total harmonic distortion (THD) of the system is calculated by applying the CSD method on the received signal.

The rest of the paper is organized as follows. In Section II, theoretical analysis on the received power and the effect of rubble EM properties on wave propagation is briefly expressed. Section III introduces mathematical theory of the optimum and null point detection in Doppler radars along with the THD calculation. The system block diagram and the rubble model are explained in Section IV. Finally, in Section V system simulation results are presented, followed by a conclusion in Section VI.

II. WAVE PROPAGATION THROUGH RUBBLE

EM properties of materials are specified by their permittivity, conductivity, and magnetic permeability. Relative permittivity and conductivity of some common building materials at L-band of microwave frequencies are available in Table I. For a plane wave propagating in an electrically conducting dielectric medium of uniform magnetic properties, the propagation constant γ, attenuation constant α and phase coefficient β are expressed by

$$\gamma = \alpha + j\beta = \sqrt{(\sigma + j\omega\varepsilon)\, j\omega\mu} \tag{1}$$

$$\alpha = \omega\sqrt{\mu\varepsilon}\left(\frac{1}{2}\left[\sqrt{1+\left(\frac{\sigma}{\omega\varepsilon}\right)^2}-1\right]\right)^{1/2} \tag{2}$$

$$\beta = \omega\sqrt{\mu\varepsilon}\left(\frac{1}{2}\left[\sqrt{1+\left(\frac{\sigma}{\omega\varepsilon}\right)^2}+1\right]\right)^{1/2} \tag{3}$$

where ω is the angular frequency, $\varepsilon = \varepsilon_0\varepsilon_r$ is the absolute permittivity, σ is the conductivity, and $\mu = \mu_r\mu_0$ is the absolute permeability [13]. ε_0 and μ_0 are attributed to the free space properties and equal to $8.85\times10^{-12}\,F/m$ and $4\pi\times10^{-7}\,H/m$, respectively. ε_r and μ_r are material's EM properties

TABLE I. EM PROPERTIES OF SOME BUILDING MATERIALS AT L-BAND OF MICROWAVE FREQUENCIES [13,14].

Material	Relative permittivity	Conductivity (S/m)
Concrete (wet)	15	0.1
Concrete (saturated)	8.5	0.05
Concrete (air dried)	4.5	0.02
Brick	3.8	0.038
Wood	2.5	0.005

compared to the free space.

Given a *z*-directed, *x*-polarized uniform plane wave incident on a planar interface of two different media located on the *x*-*y* plane, the phasor fields associated with the incident, reflected and transmitted fields may be written as

$$\begin{cases} E_s^i = E_{s_0} e^{-\gamma_1 z}\,\hat{a}_x \\ E_s^r = \Gamma E_{s_0} e^{\gamma_1 z}\,\hat{a}_x \\ E_s^t = \tau E_{s_0} e^{-\gamma_2 z}\,\hat{a}_x \end{cases} \quad (4)$$

where E_s^i, E_s^r and E_s^t are incident, reflected, and transmitted wave fields, respectively [15]. E_{s0} is the initial value of the electric field. Γ and τ are reflection and the transmission coefficients which are expressed as

$$\Gamma = \frac{\eta_2 - \eta_1}{\eta_2 + \eta_1} \quad (5)$$

$$\tau = \frac{2\eta_2}{\eta_2 + \eta_1} \quad (6)$$

where η_i is the intrinsic wave impedance of each medium which in general is a complex number. The Poynting vector defines the time-average power density vector (direction and density of power flow at a point). In general, the time-average power flow for a plane wave may be written straightforward as

$$P_{ave} = \frac{1}{2}\mathrm{Re}\left[E_s \times H_s^*\right] = \frac{1}{2}\mathrm{Re}\left[E_s H_s^* \hat{a}_k\right] \quad (7)$$

where P_{av} is the time-average power flow, $\hat{a}_k$ is the direction of Poynting vector, and H_s^* is the conjugated magnetic field. By using the relation between magnetic field and electric field in (7), the time-average power flow is obtained in W/m^2 as [16]

$$P_{ave} = \frac{\hat{a}_k}{2}\mathrm{Re}\left[\frac{E_s E_s^*}{\eta^*}\right] = \frac{\hat{a}_k}{2}\mathrm{Re}\left[\frac{|E_s|^2}{|\eta| e^{-j\theta_\eta}}\right] = \frac{1}{2}\frac{|E_s|^2}{|\eta|}\cos\theta_\eta\ \hat{a}_k . \quad (8)$$

III. Demodulation of the Received Signal

The received signal at baseband can be written as [7]

$$B(t) = \cos\left[\theta + \frac{4\pi x(t)}{\lambda} + \Delta\phi(t)\right] \quad (9)$$

where

$$\theta = \frac{4\pi d_0}{\lambda} + \theta_0. \quad (10)$$

The total residual phase noise, $\Delta\phi(t)$, is very small due to range correlation effect [11]. $4\pi d_0/\lambda$ is the constant phase shift corresponding to the nominal distance between the radar and the human body, and θ_0 is the phase shift due to reflections from other surfaces such as thick walls, rubble, and delays between circuit components. For values of θ that are odd multiples of $\pi/2$, the output is linearly proportional to $x(t)$. In this case, the output signal is at its optimum point. If θ is an integer multiple of π, the baseband signal is not linearly proportional to $x(t)$, and hence the output signal is at the null point. In other words, in some distances away from the radar transmitter, the received power reaches its minimum. These extreme cases happen every $\lambda/8$ away from the radar [11].

In order to overcome this issue, quadrature receiver for the MLDS is proposed in this paper. By using both in-phase and quadrature channels, if one channel is at the null point, the other channel will be certainly at the optimum point.

In comparison to the system proposed in [12] for the medical applications, the proposed quadrature receiver is used to find survivors trapped under rubble by overcoming the null point issue by using the channel with higher received power or by appropriate combination of two channels. Using harmonic radar in the MLDS is another low-cost method which is proposed in this work for the first time to cancel the null points which improves the sensitivity.

A: THD Calculation

To calculate the THD of the received signal, the amplitude of each frequency component of heartbeat or respiration (i.e. fundamental, 2nd, 3rd and any considerable component) at the baseband can be determined by using the CSD method [3].

The exponential received signal can be expanded using Bessel's functions to obtain the expression given by [7]

$$\begin{aligned} S(t) &= \exp\left\{ j\left[-\frac{4\pi x_h(t)}{\lambda} - \frac{4\pi x_r(t)}{\lambda} + \phi \right] \right. \\ &= dc_{IQ} + 2j\left[C_{10}\sin(\omega_r t) + C_{01}\sin(\omega_h t) + \ldots\right].e^{j\phi} \\ &+ 2\left[C_{20}\cos(2\omega_r t) + C_{02}\cos(2\omega_h t) + \ldots\right].e^{j\phi} \end{aligned} \quad (11)$$

where dc_{IQ}, the dc component, equals to $dc_I + j\,dc_Q$, ϕ is the residual phase noise due to distance between radar and trapped victim along with the unwanted reflections from other surfaces (i.e. other than the chest-wall). $x_h(t) = m_h \sin(\omega_h t)$ and $x_r(t) = m_r \sin(\omega_r t)$ are the corresponding periodic chest-wall movements due to heartbeat and respiration, respectively.

$C_{ij} = J_i\left(\frac{4\pi m_r}{\lambda}\right) J_j\left(\frac{4\pi m_h}{\lambda}\right)$ determines the amplitude of each frequency component of the baseband signal where $J_n(x)$ is the n–th order Bessel's function of the first kind [7]. The desired signals are due to the respiration and heartbeat with the movement amplitude of 0.80-10.0 mm and 0.01-0.20 mm, respectively. The respiration signal has fundamental frequency component over the range of 0.01 to 1 Hz, in comparison with 0.6 to 3 Hz for the heartbeat signal.

IV. System Model and Block Diagram

Fig. 1 presents the overall block diagram of the MLDS. A low phase noise oscillator is used to generate a stable CW signal as the transmit signal. After being amplified by a low noise amplifier (LNA), the band-pass filter (BPF) is used to filter the RF input signal. The 10 dB directional coupler keeps $9/10^{th}$ of the input signal in the transmitter path and sends $1/10^{th}$ of it to other parts of the circuit to make the clutter cancellation signal, and also provides the LO signal of the I/Q mixer. By using a digital-controlled phase shifter and an attenuator, the clutter cancellation signal is produced by the procedure explained in [17].

The transmit signal is then amplified by a power amplifier and sent through the rubble by the transmit antenna in order to find the target. It should be noted that the dual antenna system is used to reduce direct coupling between the transmitter and receiver [10].

The antenna type for the proposed system is horn for two reasons. First, the antenna gain can be up to 5 dB more than that of micro-strip patch antennas. As mentioned before, the received power is the most important issue in life-detection process. Therefore, patch antenna is unable to provide the high gain needed in the transmitter path. Second, the efficiency of horn antennas is about 10 percent better than that of the patch antennas [10].

The desired life signals and a large clutter signal due to reflections from other surfaces (i.e. rubble and thick walls) are received by the receive antenna. After filtering, clutter cancellation signal is added to the received signal by a power combiner. By adding the reflected wave to the clutter cancellation signal, which has the same amplitude of clutter but with opposite phase, the clean signal with (hopefully) no clutter is extracted. After pre-amplifying, this signal is fed to RF port of the in-phase/quadrature mixer. The LO port of the mixer is fed by the same transmitter source. The phase shifter before the LO port of mixer reduces the phase difference between the LO and RF port to zero in order to obtain the maximum sensitivity. In-phase and quadrature channels will then be sent to the processing unit after low-pass filtering. The channel with higher quality (i.e. not located at the null points) or an appropriate combination of both channels will then be processed to extract the life signals. Fig. 2 presents the proposed harmonic radar structure that can be used instead of conventional transmitter architectures in the MLDS. This structure shows a significant improvement in null points cancellation [18]. The harmonic radar in Fig. 2 uses the fundamental and harmonic carrier frequencies (usually the second harmonic) instead of a single carrier to transmit the signal through the rubble by two antennas with different center frequencies. All circuit components (except for the antennas) are able to work at both the fundamental and the harmonic carrier frequencies. By using a phase shifter (φ) before one

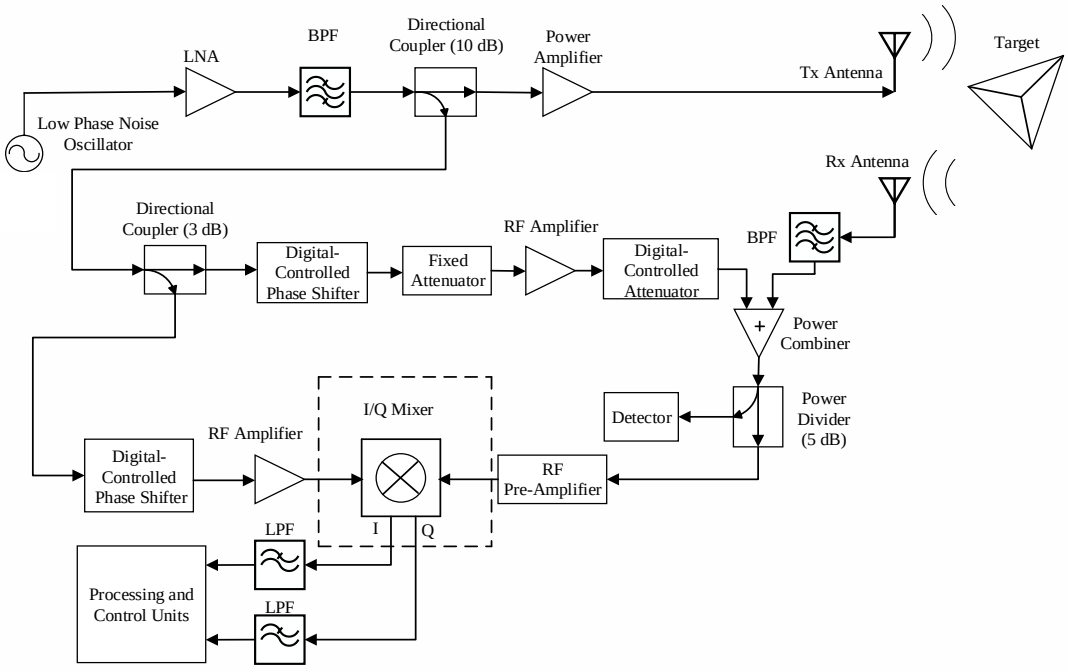

Figure 1. Complete block diagram of the MLDS.

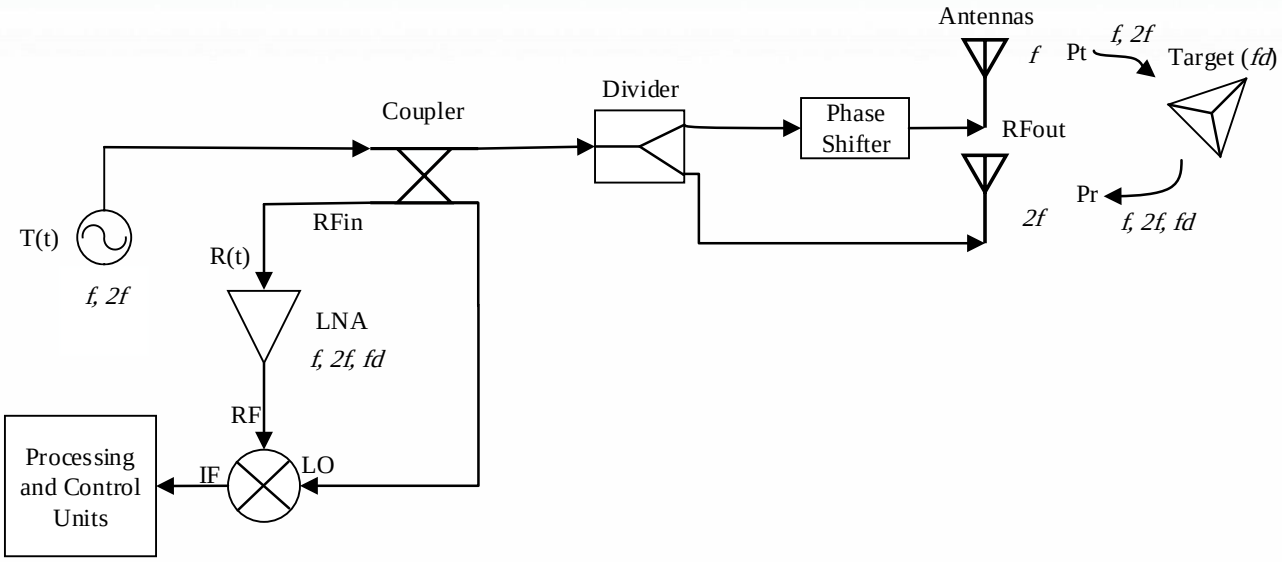

Figure 2. The proposed harmonic radar transceiver architecture used in the MLDS.

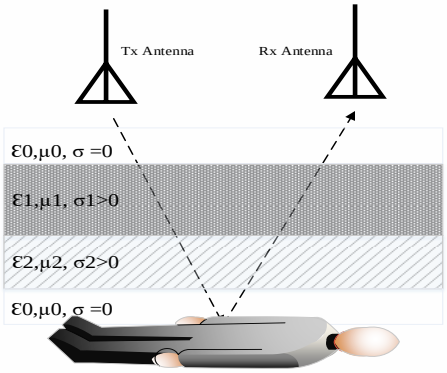

Figure 3. Rubble simulation model.

of the antennas, the system can be able to completely cancel the null points and hence improve the received power of the system. Simulations in Section V are performed to show the performance improvements of harmonic radar for the MLDS.

Fig. 3 demonstrates a simple rubble simulation model to estimate the received power of the MLDS. For simplicity, rubble slabs are considered on the top of each other without any angle. For the life signals to be detectable, the received power should be higher than the noise floor which is dominated by the flicker noise [18]. Simulations are performed in Section V to compare the received power in free space and in the presence of rubble model used in this paper.

V. Results and Discussions

To verify theoretical analysis, software tools are used to perform system-level simulations. CW Doppler radar is implemented in order to assess the THD performance of system. Also, EM propagation in the rubble medium is analyzed for different conditions.

A: Spectral Analysis of the MLDS

Output spectra of the proposed system for two different operating frequencies are demonstrated in Fig. 4 by implementing the block diagram of a single carrier system explained in Fig. 1. Fig. 4 (a) shows the output spectrum when no target exists and no life signals are available to be detected. Output spectrum of the in-phase channel in Fig. 4 (b) shows two fundamental frequency components of respiration and heartbeat of the target at 0.37 Hz and 1.2 Hz, respectively. These values are the corresponding respiration rate (RR) of 22 bpm and heartbeat rate (HR) of 72 bpm. Also, carrier frequency of the MLDS is 1.15 GHz, the same as the system proposed in [10].

Fig. 4 (c) shows the output spectrum of the MLDS at 10 GHz carrier frequency. It is clear from the results that harmonics are more noticeable in higher frequencies. At 10 GHz, the amplitude of respiration 2nd harmonic at 0.74 Hz (-7 dBm) is almost equal to that of the heartbeat fundamental frequency component at 1.2 Hz. Moreover, there is about 19 dB difference between desired signals in two operating frequencies which proves higher sensitivity of the system at higher frequencies. Note that the distance between the radar and the target is about 5 m in both setups.

B: EM Wave Propagation through Rubble

Fig. 5 shows EM wave attenuation and the resultant received power in the presence of a concrete layer between the radar and human target at different operating frequencies. By using EM properties of concrete experimented in [14,19], the effects of concrete conditions on the received power of the MLDS is evaluated and demonstrated in Fig. 5 (a).

In order to estimate the penetration depth of the MLDS, the received power is calculated by the procedure explained in Section II. By using the simulation parameters in Table II, the received power can be calculated by (8). For the desired signals to be detectable, the received power should be above the noise floor which is dominated by the flicker noise. For the proposed L-band radar, the flicker noise level is

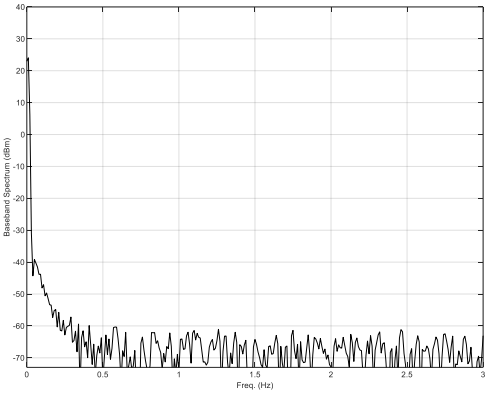

(a)

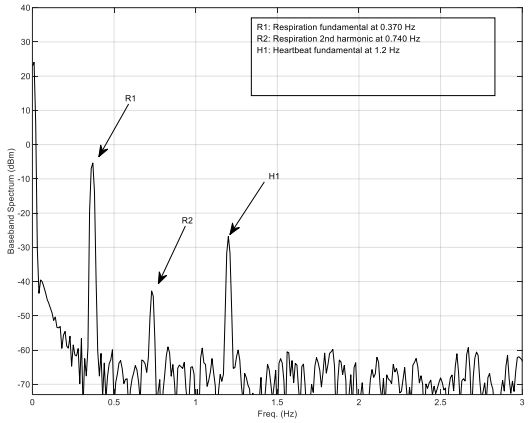

(b)

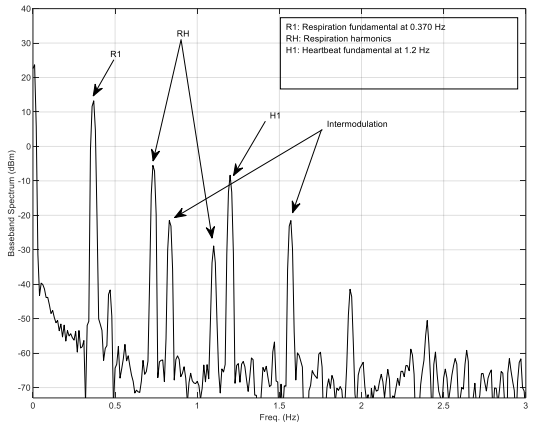

(c)

Figure 4. Output spectra of MLDS. (a) with no target under rubble (b) at 1.15 GHz carrier frequency (c) at 10 GHz carrier frequency.

about -110 dBm according to [20].

Fig. 5 (a) shows the significant effect of the moisture and the carrier frequency on the penetration depth of the radar. Simulation results show that the penetration depth in a wet concrete layer is approximately 1.5 m, while this value in air dried concrete is up to 4 m.

TABLE II. SIMULATION PARAMETERS [10].

Parameter	Value
Transmitter power	26.5dBm (446 mW)
Antenna gain	12 dBi
Electric field strength	100 V/m
Magnetic field strength	3.866 A/m
Carrier frequency (single carrier system)	1.15 GHz
Carrier frequency (harmonic system)	1.15/2.3 GHz
Distance between the MLDS and the trapped victim	1-5 m

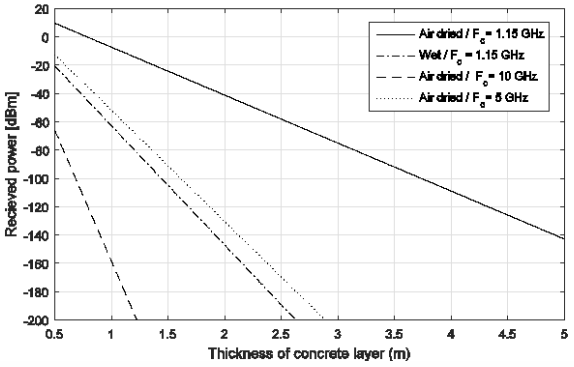

(a)

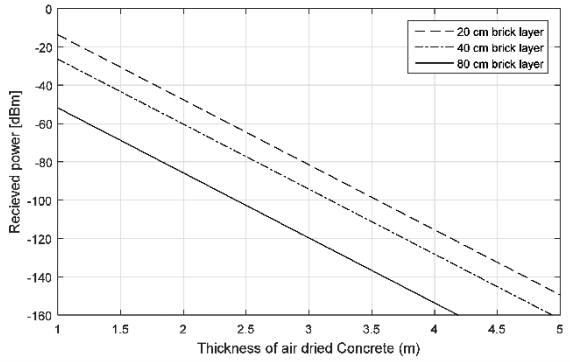

(b)

Figure 5. The received power in the presence of a concrete layer between radar and human target. (a) one layer of concrete (b) two-layer rubble.

The penetration depth can be significantly reduced at higher frequencies due to increase in conductivity of the building materials [13]. Hence, in order to obtain the penetration depth up to 5 m, the use of L-band carrier frequency is crucial. It should be noticed that in the presence of reinforced concrete layer and metallic wire mesh between the MLDS and the target, the 1.15 GHz transmitted wave can penetrate easier than the 450 MHz EM wave [4]. Moreover, by

examining the results of Subection A, it is clear that using frequencies lower than 1.15 GHz as the carrier frequency can considerably degrade the sensitivity of the system. Consequently, superiority of 1.15 GHz, as the minimum carrier frequency, is proven. The received power loss of the radar signal at 1.15 GHz in wet and air dried concrete are approximately 80 dB/m and 35 dB/m, respectively.

To obtain more realistic results, in another scenario, different layers of building materials as the rubble are considered by using Table I. An additional brick layer is considered under the air dried concrete slab in order to model the two-layer rubble between the MLDS radar and the trapped victim. Thickness of brick layers is assumed to be 20 cm, 40 cm, and 80 cm, respectively, while the thickness of concrete slab varies between 1 to 5 m. Results in Fig. 5 (b) show that the penetration depth in this cases is reduced up to 0.5 m.

In order to compare the results, the received power of a single carrier system is depicted in Fig. 6 (a) while both the MLDS and the target are in free space. For a 26.5 dBm transmit power, the received power at 1.15 GHz is about -40 dBm for a distance of about 5 m.

The null points issue which was explained in Section III is considered in Fig. 6 (a). By using the harmonic radar structure with dual carrier in the MLDS, null points can be reduced or completely cancelled. Fig. 6 (b) shows the received power when the phase shifter before the transmit antenna at the 1.15 GHz center frequency is set to zero ($\varphi = 0$) while both transmit signals are in-phase. It is clear that all null points are cancelled and the received power will not be significantly reduced. Fig. 6 (c) shows the received power for $\varphi = 45$ where clearly the number of null points in this case is significantly less than that of a single carrier system. Results show that by using a digitally controlled phase shifter before one of the transmit antennas in the harmonic radar structure, the MLDS system can be able to change the phase difference between the transmit signals automatically and obtain the maximum performance.

C: Signal Demodulation and THD Calculation

Signal demodulation and the CSD method were described in Section III. By using (11), the amplitude of each frequency component of heartbeat and respiration signals can be derived using Bessel's functions. Respiration and heartbeat signals are considered as two sine waves of 0.37 Hz and 1.2 Hz, respectively.

Fig. 7 (a) shows the amplitude of each frequency component of the received signal at different operating frequencies. As mentioned before, the amplitude of the received signal increases at higher frequencies which leads to a better sensitivity. Fig. 7 (b) shows the ratio between the heartbeat and the nearest (and most often the highest) interferer, the third harmonic of the respiration signal. Four different levels are considered for the respiration signal to demonstrate its effect on the heartbeat signal. Results show that for the amplitudes about 1.8 mm, the third harmonic of respiration can considerably affect on the heartbeat fundamental frequency for frequencies higher than 10 GHz.

Fig. 8 shows the distribution of null points in the received signal at two different operating frequencies for both the in-phase and the quadrature channels. The amplitude of the fundamental component and the 2nd harmonic of respiration and fundamental heartbeat signal for a system with 1.15 GHz carrier frequency are demonstrated in Fig. 8 (a). It is clear that when the in-phase channel is at the null point, the quadrature

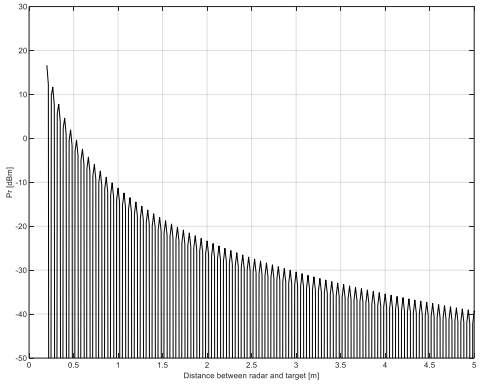

(a)

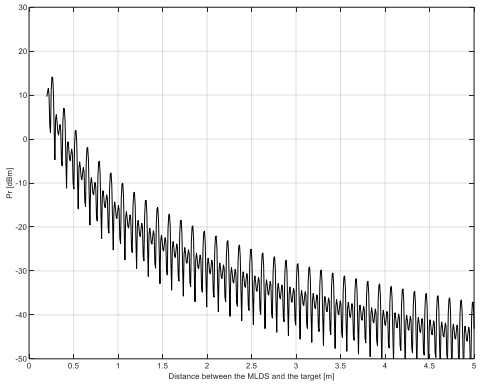

(b)

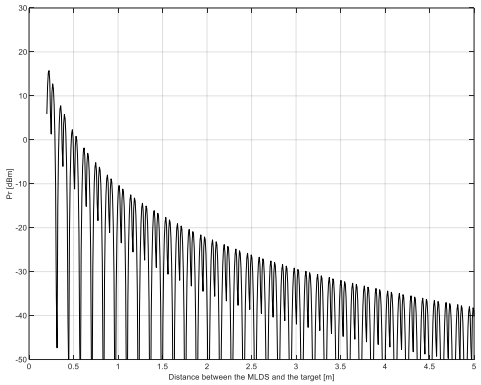

(c)

Figure 6. The received power in free space. (a) conventional single carrier system (b) harmonic system with $\varphi = 0$ (c) harmonic system with $\varphi = 45$.

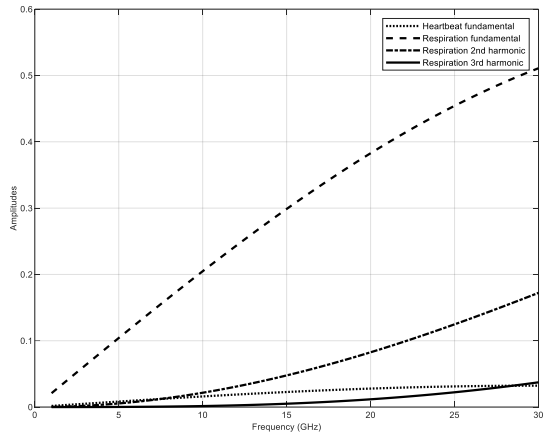

(a)

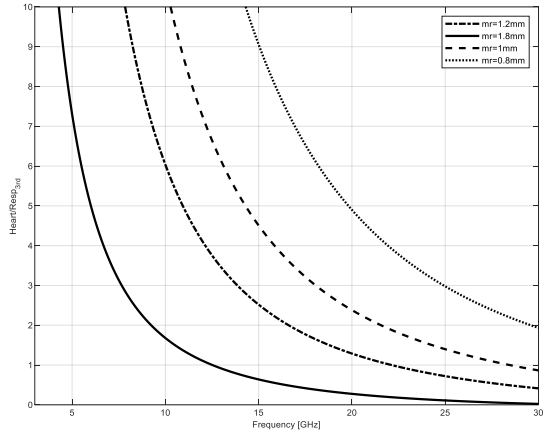

(b)

Figure 7. Amplitude of demodulated signals (a) amplitude of each frequency components of the received signal (b) the ratio between the heartbeat and the third harmonic of respiration signal.

channel is at the optimum point. Consequently, by using just one channel, the MLDS could not be able to detect the victim located at null points, hence using both channels are crucial. Results show that at 1.15 GHz, null points occur each 6.52 cm ($\lambda/4$) away from the MLDS. However, at 10 GHz carrier frequency, this value is about 7.5 mm as demonstrated in Fig. 8 (b).

Fig. 9 shows the distribution of null points, obtained by using the CSD method, when the harmonic radar structure is used in the MLDS. For better comparison, the amplitude of respiration signal for both the single carrier and dual carrier (harmonic) systems are considered in Fig. 9. The distribution of null points is shown in Fig. 9 (a) for $\varphi = 0$. In this case, the null points of the single carrier system (1.15 GHz) at distances of 5 and 11.52 cm are cancelled. In addition, because of increase in the amplitude of the respiration signal, the

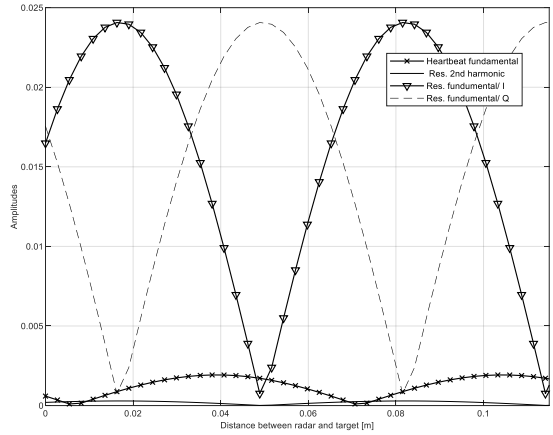

(a)

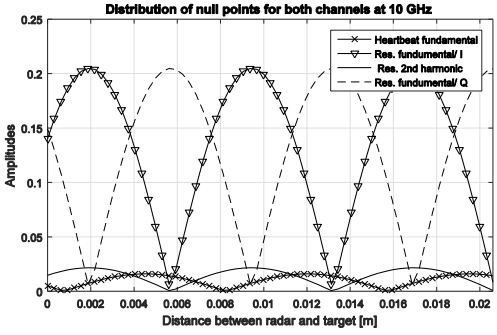

(b)

Figure 8. Distribution of null points for both channels at two different operating frequencies (a) 1.15 GHz (b) 10 GHz.

sensitivity of the MLDS will be improved. Also, Fig. 9 (b) shows the amplitude of respiration signal for $\varphi = 22.5$. It is clear that in this case, the null points are completely cancelled and the sensitivity of the system is improved. Therefore, using a digitally-controlled phase shifter before one of the transmitting antennas is crucial.

In order to describe MLDS performance at different frequencies by using the CSD method, (12) is used to calculate the THD;

$$THD = \left(\frac{\sqrt{(V_2^2 + V_3^2 + V_4^2 + \cdots + V_n^2)}}{V_1} \right) \times 100 \qquad (12)$$

where V_i is the amplitude of i^{th} harmonic of the heartbeat or respiration signal.

Fig. 10 depicts the THD of the MLDS in different carrier frequencies. Results show that for a system with 1.15 GHz carrier frequency, the THD of the output signal is about 3 percent, while this value for a system with 10 GHz carrier frequency is about 10 percent. The THD at higher carrier frequencies is calculated in order to make the best decision in choosing the appropriate operating frequency. Also, there is almost a linear relation between the THD and the carrier frequency.

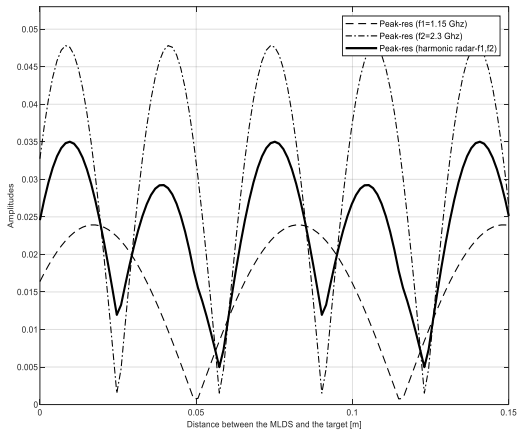

(a)

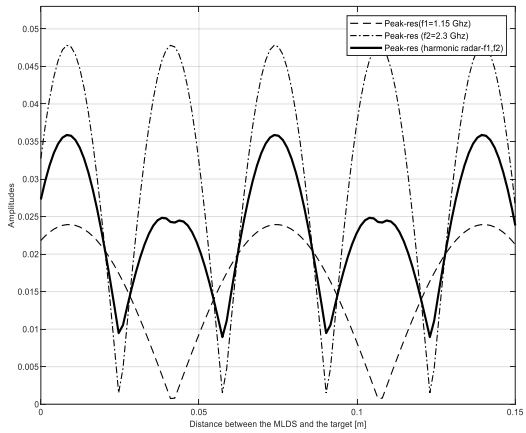

(b)

Figure 9. Distribution of null points in the harmonic system (a) $\varphi = 0$ (b) $\varphi = 22.5$.

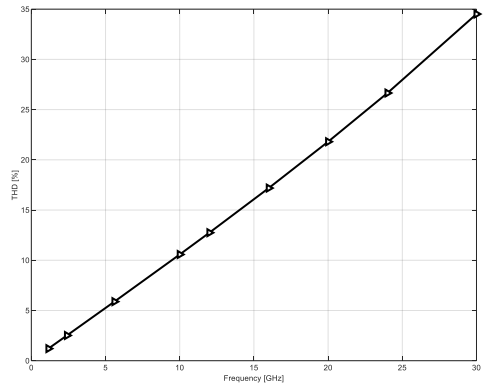

Figure 10. THD of the output signal at different carrier frequencies.

VI. CONCLUSION

Performance assessment of the proposed MLDS shows that one noticeable receiver architecture can be the quadrature receiver which resolves detection uncertainty caused by null points. Harmonic radar structure is another low-cost method to cancel the null points which therefore improves the sensitivity of the MLDS. However, in order to obtain the maximum performance, employing a digitally-controlled phase shifter prior to one of the antennas in the harmonic radar is crucial. Effect of different layers of building rubbles and moisture on the penetration depth of the radar signal is evaluated by considering different conditions for concrete. Results show that the received power reduction in wet concrete is up to 80 dB/m. Appropriate operating frequency is determined by comparing the THD of the system. By examining different frequencies, 1.15 GHz (L-band) is found to be the most appropriate one because of better penetration depth of about 5 m in common building materials and lower THD of about 3 percent. Also, 1.15 GHz as the minimum carrier frequency was selected by performing several simulations and observing the penetration depth of the MLDS at different frequencies.

REFERENCES

[1]. K.M. Chen, D. Misra, ” Wang, H., et al. ”An X-band microwave life-detection system”. IEEE Transactions on Biomedical Engineering, 1986, no. 7, pp. 697-701

[2]. B.K. Park, O. Boric-Lubecke, V.M. Lubecke, “Arctangent demodulation with DC offset compensation in quadrature Doppler radar receiver systems”. IEEE transactions on Microwave theory and techniques, 2007, vol. 55, no. 5, pp. 1073-1079

[3]. C. Li and J. Lin, “Complex signal demodulation and random body movement cancellation techniques for non-contact vital sign detection”. IEEE MTT-S International Microwave Symposium Digest, 2008, pp. 567-570

[4]. K.M. Chen, Y. Huang, J. Zhang, et al. , “Microwave life-detection systems for searching human subjects under earthquake rubble or behind barrier”. IEEE transactions on biomedical engineering, 2000, vol. 47, no. 1, pp. 105-114

[5]. C. Li, V.M. Lubecke, O. Boric-Lubecke, J. Lin, “A review on recent advances in Doppler radar sensors for noncontact healthcare monitoring”. IEEE Transactions on microwave theory and techniques, 2013, vol. 61, no. 5, pp. 2046-2060

[6]. M. Pieraccini, G. Luzi, D. Dei, et al., “Detection of breathing and heartbeat through snow using a microwave transceiver”. IEEE Geoscience and Remote Sensing Letters, 2008, vol. 5, no. 1, pp. 57-59

[7]. J. Tu, T. Hwang, J. Lin, “Respiration rate measurement under 1-D body motion using single continuous-wave Doppler radar vital sign detection system”. IEEE Transactions on Microwave Theory and Techniques, 2016, vol. 64, no. 6, pp. 1937-1946

[8]. M. Donelli, “A rescue radar system for the detection of victims trapped under rubble based on the independent component analysis algorithm”. Progress In Electromagnetics Research M, 2011, vol. 19, pp. 173-181

[9]. H.R. Chuang, H.C. Kuo, F.L. Lin, et al. “60-GHz millimeter-wave life detection system (MLDS) for noncontact human vital-signal monitoring”. IEEE Sensors Journal, 2012, vol. 12, no. 3, pp. 602-609

[10]. F. Jalali Bidgoli, S. Moghadami, S. Ardalan, “A Compact Portable Microwave Life-Detection Device for Finding Survivors”. IEEE Embedded Systems Letters, 2016, vol. 8, no. 1, pp. 10-13

[11]. A.D. Droitcour, O. Boric-Lubecke, V.M. Lubecke, et al. “Range correlation and I/Q performance benefits in single-chip silicon Doppler radars for noncontact cardiopulmonary monitoring”. IEEE Transactions on Microwave Theory and Techniques, 2004, vol. 52, no. 3, pp. 838-848

[12]. C. Li, Y., Xiao, J. Lin, “Experiment and spectral analysis of a low-power Ka-band heartbeat detector measuring from four sides of a human body”. 2006, IEEE Transactions on Microwave Theory and Techniques, vol. 54, no. 12, pp. 4464-4471

[13]. H.M. Jol, “Ground penetrating radar theory and applications”. Elsevier, 2008.

[14]. O. Buyukozturk, “Electromagnetic Properties of Concrete and Their Significance in Nondestructive Testing” Transportation Research Record: Journal of the Transportation Research Board, 1997, vol. 1574 pp. 10-17

[15]. Ø. Aardal, Y. Paichard, B. Sverre, T. Berger, et al., "Physical working principles of medical radar", IEEE Transactions on Biomedical Engineering, 2013, vol. 60, no. 4, pp. 1142-1149
[16]. C.T.A. Johnk, "'Engineering electromagnetic fields and waves". New York, John Wiley and Sons, Inc., 1975.
[17]. Y. Zhang, Z. Li, T. Jiao, et al., "Simulation research of microwave automatic clutter-cancellation in life-detection radar". 3rd International Conference on Biomedical Engineering and Informatics (BMEI), 2010, vol. 5, pp. 2098-2100
[18]. L. Chioukh, H. Boutayeb, D. Deslandes, et al., "Noise and sensitivity of harmonic radar architecture for remote sensing and detection of vital signs". IEEE Transactions on Microwave Theory and Techniques, 2014, vol. 62, no. 9, pp. 1847-1855
[19]. D. Pena, R. Feick, H.D. Hristov, et al., "Measurement and modeling of propagation losses in brick and concrete walls for the 900-MHz band". IEEE Transactions on Antennas and Propagation, 2003, vol. 51, no. 1, pp. 31-39
[20]. D. Nguyen, S. Yamada, B.K. Park, et al., "Noise considerations for remote detection of life signs with microwave Doppler radar". 29th Annual International Conference of the IEEE in Engineering in Medicine and Biology Society (EMBS), 2007, pp. 1667-1670.

Kamyar Abyar Langroudi received his B.Sc. and M.Sc. degrees from the University of Guilan, Iran, in 2015 and 2017, in Electrical and Telecommunications Engineering, respectively. His research interests are focused on Ultra Wideband (UWB) radars and microwave propagation systems.

Gholamreza Baghersalimi received his B.Sc. degree from the University of Tehran, Iran, M.Sc. degree from Tarbiat Modares University, Iran, and Ph.D. degree from Leeds University, UK, all in Electrical Engineering. Now, he is an Associate Professor in the Department of Electrical Engineering, the University of Guilan. He has served as the Head of the Department of Electrical Engineering, Pro-Dean for Academic Affairs, and Pro-Dean for Research Affairs at the Engineering Faculty. He has also served as Reviewer of the Journal of IET Communications, IEEE Access, International Journal of Communication Systems (IJCS), International Journal for Light and Electron Optics (Optik), Transactions on Emerging Telecommunications Technologies (Wiley), and Radioengineering. His research interests are focused on physical layer signal processing techniques in fiber-optic communication systems, optical wireless communications especially visible light communications. He has published over 50 journal and conference papers and graduated over 50 M.Sc. students.

Alireza Saberkari received the M.Sc. (Hons.) and Ph.D. (Hons.) degrees in electrical engineering from Iran University of Science and Technology, Tehran, Iran, in 2004 and 2010, respectively. Since 2010, he has been with the Department of Electrical Engineering, University of Guilan, Rasht, Iran, where he became an Associate Professor in 2015. He is the Director of the Microelectronics Research Lab, University of Guilan. During the period 2008–2009, he joined to the group of Energy Processing Integrated Circuits, Technical University of Catalunya, Barcelona, Spain, as a Visiting Scholar. He has been involved in different national and international projects. His research interests include the areas of analog, RF, and mixed-signal microelectronics with particular interest in on-chip power management circuits, analog circuits for energy harvesting applications and biomedical implants, linear and low-dropout regulators (analog, digital, and hybrid), wireless energy and power transfer, current-mode circuit design, CMOS LNAs and RF power amplifiers

Mahdi Nassiri received his B.Sc. and M.Sc. degrees from the University of Guilan, Iran, in 2015 and 2017, respectively, all in Electrical Engineering. His research interests are focused on physical layer signal processing techniques in Optical Wireless Communications (OWC), Visible Light Communications (VLC), Visible Light Positioning (VLP), Multicarrier Communications, Indoor Positioning Systems (IPSs), Machine Learning (ML), Deep Learning (DL) and Neural Networks (NNs). He has m published nine journal and conference papers in these areas so far.